Brilliant Engineering 3 (2020) 16-21

Brilliant Engineering

www.acapublishing.com

RESEARCH ARTICLE

A Finite Element Analysis of The Indentation of an Elastic-Work Hardening Double Layered Half-Space by a Rigid Sphere

Hikmet Altun*, Sadri Şen
Engineering Faculty, Department of Mechanical Engineering, Ataturk University, 25030, Erzurum, Turkey

Abstract

In this work, the stresses caused by an elastic sphere indenting double layered coating on an elastic-work hardening substrate with a relatively low elastic modulus regime have been examined. An axisymmetric finite element mesh was set up for the stress analysis. The contact stress arising on the free surface, the stresses at both interface sides of the first and second coating layers and at the symmetry axis, and the stresses within the coating layers have been examined depending on the first coating layer (interlayer) thickness using ANSYS. It was obtained that the thickness of the first coating layer affected considerably the stresses formed at the contact surface, the interfaces, the symmetry axis and within the coating layers.

Keywords: Indentation, Double layered coating, Finite element.

1.Introduction

Hard coatings on relatively soft substrates and their industrial applications have been receiving more and more attention during the past few decades. The coating industry has advanced considerably in the production of various kinds of coatings to cope with the increasing number of applications of hard-coated systems. Hard coatings are usually applied to relatively soft substrates to enhance reliability and performance. Hard ceramic coatings, for example, are used as protective layers in many mechanical applications. Such coatings are usually brittle and subject to fracture of the coating or failure of the interface with the substrate. Therefore, the enhancement gained by the coatings is always accompanied by the risk of such failure.

Indentation is one of the traditional methods to quantify the mechanical properties of materials. Several techniques have been reported in the literature to extract the mechanical properties of both homogeneous and composite or coated materials from indentation experiments. Indentation has also been advocated as a tool to characterize the properties of thin films or coatings. At the same time, for example for hard wear-resistant coatings, indentation can be viewed as an elementary step of concentrated loading. For these reasons, many experimental as well as theoretical studies have been devoted to indentation of coated systems during recent years [1]

Historically, a sharp indenter has been used to determine the properties of relatively brittle materials in addition to common applications such as determination of hardness and elastic modulus. A sharp indenter such as of Berkovich type can be used to study brittle fracture behaviour of a material by investigation of the radial crack generated from the edges of the contact [2]. Spherical indenters, on the other hand, have usually been used for research on the yielding and elasto-plastic deformation behaviour of ductile materials because a spherical indenter induces a larger area of contact at a given indentation depth. Thus it is useful in studying the transition from an elastic regime to a plastic one and the elasto-plastic behaviour of a film, including strain hardening. In spherical nano-indentation, the stress concentration near the tip of the indenter is reduced significantly compared with the case of a sharp indenter. Therefore, the spherical indenter has an advantage in obtaining accurate data before crack initiation in a film or delamination at a film/substrate interface. A further notable aspect of the research on spherical indentation is that it can provide useful information to understand some phenomena taking place in sharp indentation, such as tip rounding, which are treated as error sources in analysing experimental data. A reasonable understanding of the effect of these phenomena on the experimental data is possible via a study of the spherical indentation process. As a result, the use of spherical indenters is increasing [3].

It is well-known fact that the useful layer life depends on either detachment of the coating, adhesive failure, or fracture of the layer, cohesive failure, rather than conventional wear. Cohesive failure results from stresses within the layer and at the surface, while adhesive failure occurs due to interface stresses. When designing such contacting layered material systems, it is important to have a comprehensive knowledge about the nature and the origin of these stresses for minimizing the strain fields of layered materials. Furthermore, the magnitude and distribution of the interfacial stresses, the mechanical reliability, and the analysis of contact failures are also necessary to be assessed [4].

*Corresponding Author: haltun@atauni.edu.tr
(H. Altun ORCID: 0000-0002-3738-033X)
Received 17 Dec 2019 Revised 18 Dec 2019 Accepted 18 Dec 2019
Brilliant Enginering 3 (2020) 16-21
https://doi.org/10.36937/ben.2020.003.003

There exists a series of work [5, 6, 7, 8, 9, 10, 11, 12] relating analytical and numerical solutions in this area. Komvopoulos [5] presented a study for a rigid cylinder indenting a stiff layer on an elastic substrate and it was shown that the plastic deformation in the substrate could be avoided by increasing the ratio of the layer thickness to the half-width of the contact. In other work, Komvopoulos [6] also found that the size and location of plastic zones depended strongly on the layer thickness. Kral et al. [7, 8] presented a finite-element analysis of repeated indentation of an elastic-plastic layered medium by a rigid sphere for surface [7] and subsurface [8]. Their model had a perfectly adhering layer using two different thicknesses and elastic modulus and yield stress two and four times greater than those of the substrate. Finite-element analysis for multi-layer contact under axisymmetric loading has been performed by Tangena and Wijnhoven [9]. They investigated the correlation between mechanical stresses and wear in a layered system. Tian and Saka [10] analyzed the contact problem of a rigid cylinder indenting an elastic-plastic two-layer half-space used in electrical contacts using finite-element analysis. They quantitatively addressed to the mechanism of crack initiation at the interfaces and interfacial delamination.

Although single layer coatings suit well a wide range of applications in many sectors of engineering, there is an increasing number of sectors where the properties of a single material are not sufficient. Thus, there is a need to find coatings that are better suited to such applications. One way to overcome this problem is to use a multilayer coating that combines the attractive properties of several materials. The technologically and economically significant aims of these coatings are the improvement of wear resistance, decrease of friction coefficient and betterment of corrosion protection [13]. There is great interest in developing techniques to optimize coating adhesion. A variety of approaches may be exploited for this purpose, including selecting coating and substrate materials with appropriate elastic and plastic properties, optimizing the thickness of the coating, and modifying the chemistry of the coating/substrate interface itself [14].

In this work, to investigate the effect of the thickness of the interlayer at the double layered coatings on the stress distribution, the stresses caused by an elastic sphere indenting double layered coating on an elastic-work hardening substrate with a relatively low elastic modulus regime have been examined. An axisymmetric finite element mesh was set up for the stress analysis. The contact stress arising on the free surface, the stresses at both interface sides of the first and second coating layers and at the symmetry axis, and the stresses within the coating layers have been examined depending on the first coating layer (interlayer) thicknesses using ANSYS. Then, it was studied to determine the probable crack initiating places at the coating system.

2. Statement of problem

The system considered in this study is illustrated in Fig.1a. It comprises an elastic-plastic, work hardening substrate coated two elastic layers and indented by a rigid spherical indenter. The indenter has a radius of 10 mm. The problem was modeled using a finite element method, and boundary conditions and meshing are given in Fig.1a and Fig.1b. Assuming the problem is axisymmetric, with radial coordinate r and axial coordinate y in the indentation direction, as illustrated in the Figure 1.

Boundary conditions were expressed in the following.

$$\sigma_y(r,0)=0 \qquad |r|>a \tag{1}$$

$$\tau_{r\theta}(r,0)=0 \qquad -\infty<r<\infty \tag{2}$$

where a is the radius of the contact area.

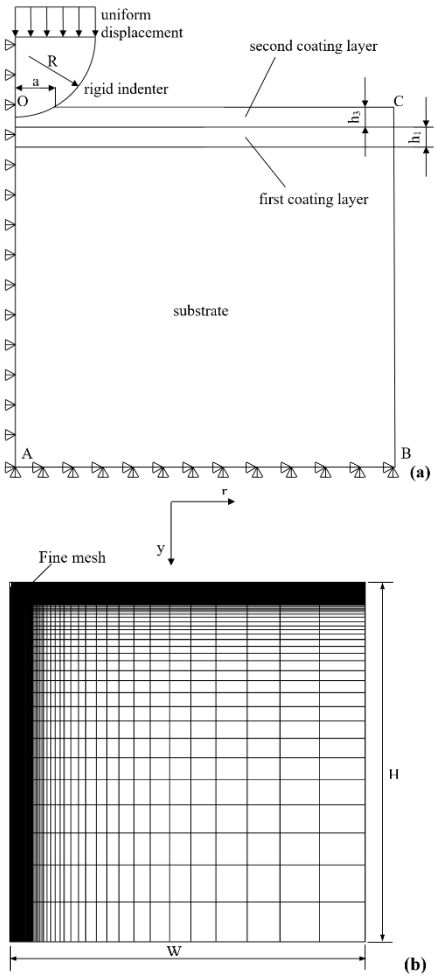

Figure 1. (a) The finite element model and the boundary conditions (b) The solution mesh

Perfect bonding is assumed at the interfaces between both two coating layers and the substrate and first coating layer, i.e. displacements across the interfaces are continuous

$$u^{(1)}(r,h2)=u^{(2)}(r,h2) \tag{3}$$

$$u^{(1)}(r,h1+h2)=u^{(3)}(r,h1+h2) \tag{4}$$

$$v^{(1)}(r,h2)=v^{(2)}(r,h2) \tag{5}$$

$$v^{(1)}(r,h1+h2)=v^{(3)}(r,h1+h2) \tag{6}$$

$$u=v=0 \quad \text{as} \quad r,y \rightarrow \infty \tag{7}$$

where the superscripts 1, 2 and 3 present the first coating layer, the second coating layer and the substrate, respectively, and h1 and h2 are the layer thicknesses of the first and second coating layers, respectively. The materials for the layers and the substrate are assumed to possess linear elastic and bilinear elastic-plastic behaviour, respectively, and the material curve of the substrate is given in Fig.2. All the material properties are listed in Tables 1 and 2.

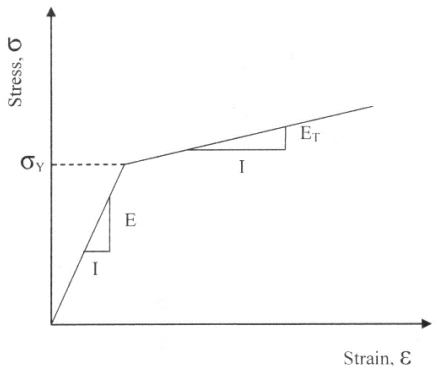

Figure 2. Bilinear elastic-plastic behaviour of the substrate material ($ET=\alpha E$)

Table 1. Mechanical properties of contact materials

Material	Young's modulus E(GPa)	Poisson's ratio, n	Yield strength, σ_y (MPa)	$E_T/E,\alpha$
Indenter	rigid	-	-	-
Substrate	220	0.30	220	0.1
First coating layer	400	0.25	-	-
Second coating layer	600	0.25	-	-

Table 2. Load and geometrical parameters used in stress analysis

Radius of indenter	R	10 mm
Normal constant load (as displacement)	d	1 mm
Thickness of the first coating layer	h1	0.10, 0.30, 0.50, 0.75, 1 mm
Thickness of the second coating layer	h2	0.50 mm
Radius of the model in r direction	W	100 mm
High of the model in y direction	H	100 mm

Young's moduli were chosen 220, 400 and 600 GPa for the substrate, first coating layer and second coating layer, respectively. Young's modulus for the substrate has been chosen as 220 GPa similar to that for steel. The range of 200-800 GPa covers the moduli of ceramic coatings which are likely of interest for tribological applications (Sen et al., 1998). To investigate the effect of the thickness of the first coating layer, h1, on contact stress arising on the free surface and at interface sides of the first and second coating layers and the stresses at the symmetry axis, the thickness of the second layer, h2, was kept constant as 0.50 mm, and h1 was changed.

3. The finite element model

To carry out the finite element analysis for the indentation of a spherical indenter on the double layered half-space, the axisymmetric dimensions in the half-space are modelled using the axes of r and y. The boundary conditions of the present model are illustrated in Fig.1(a). Because of the load symmetry and the axisymmetric geometry, only half of the layered media was considered. The mid-plane (OA) was restricted to move only along the y-direction. The displacements at the bottom of the block (AB) are far away from the contact and are assumed to be zero in the vertical and horizontal directions. Fig.1(b) is the whole finite element mesh.

Two-dimensional four-node quadrilateral axisymmetric isoparametric solid elements were used for the layers and the substrate in the finite element model. The number of the elements and nodes was constant in the second coating layer and the substrate. The number of the elements and nodes are 2000 and 1862, respectively, in the second coating layer, and are 9000 and 8624, respectively, for the substrate. The numbers of nodes and elements in the first coating layer was increased with increase in the coating thickness of the first layer, and are given in Table 3. The horizontal and vertical dimensions of the mesh are both 100 mm, which is large enough to allow the stresses and the displacements to be insignificant at the boundaries. The interfaces between both two layers and the substrate and first layer were assumed to be perfectly bonded, i.e. the displacements at interface were continuous (Eqs. (3)-(6)). These interface constraints were satisfied by using common nodes which belong to the elements on both sides. The normal contact between the rigid sphere and the layered half-space was modeled with a two-dimensional point to ground axisymmetric interface (gap) elements of ANSYS. The initial nodal gaps between the rigid spherical indenter and the surface of the layered half-space were prescribed by the circumference of the indenter. The ANSYS finite element program detects the gap changes and indicates the gap closure by following the position of points on one surface relative to the lines (or areas) of another surface in y and r directions. Whenever the closure distance becomes zero at any node, then contact is assumed to occur and an external reaction force is exerted on that node; otherwise no force is transferred. The parameter associated with the interface elements, the "friction coefficient", is assumed to be zero.

Table 3. The layer thicknesses and the number of the elements and the nodes in the first coating layer used in the FEM model

Layer thickness (mm)	The Number of the elements and the nodes of the first coating layer	
	Element	Node
0.10	400	294
0.30	1200	1078
0.50	2000	1862
0.75	3000	2842
1	4000	3822

Mesh refinements were included to predict accurately the stress distributions at the interface, the contact surface and the symmetry axis because highly stressed regions was near the contact area (Fig. 1(b)). Hence, the closest spacing of nodes is immediately beneath the contact surface.

To simulate indentation, a specified displacement was applied to the top surface of the indenter. Indentation was simulated by imposing small incremental displacements to the nodes on the upper line of the indenter seen in the Fig. 1(a). The nodes of the midplane ($r=0$) along y-axis were restricted to move only along the y-direction. The displacements at the bottom plane of the block (AB) are far away from the contact and are assumed to be zero in the vertical and horizontal directions. Loading process was modelled through a series of load steps, and twenty load steps at the loading stage were used to assign a maximum vertical displacement of 1 mm to the nodes on the upper line of the indenter.

To check the validity of the finite element solution, the stress distribution from numerical results obtained for the special indentation of a homogeneous elastic half-space are checked against

the known exact Hertzian solution. The difference between the numerical results obtained using the FEM and the corresponding analytical solution was found to be less than 0.1%. It may be concluded, therefore, that the finite-element mesh used in this work is an acceptable representation of an elastic semi-infinite solid.

4. Results and Discussion

In this study, all the current calculated stresses have been presented in a normalized form because the stresses are usually normalized by the maximum hertzian pressure of the contact in the elastic stress analysis of the homogeneous media. The stresses were normalized with respect to the center pressure, *p**, of the homogeneous model depending on the appropriateness. Here, positive and negative values indicate tensile and compressive stresses, respectively. The vertical distance *y* below the contact was normalized for each model by the thickness of the related coating layer. Thus, for the stress distribution along the loading (symmetry) axis, both the interfaces between the coating layers and the first coating layer-substrate were brought to the same *y/y** values. The radial distances were normalized by the radius of the contact zone, a. The stresses were normalized by the center contact pressure p*(σy) under the load applied to all models.

The stresses at the contact surface, at the interfaces between both coating layers and coating layer-substrate, and at the symmetry axis are very important. The stress components relevant to the analysis are: tensile in-plane stresses, which can cause brittle failure of the film at its surface and interface or coating detachment; high compressive in-plane stresses, which can cause buckling of the film in the presence of interfacial crack and local areas of poor adhesion.

Fig.3 shows normalized radial stress, σ_r, distributions at the contact surface for various layer thicknesses of the first coating layer. It is seen in the figure that the radial stress is compressive in the contact zone (*r/a<1*), until near the outside of the contact zone, and then becomes tensile. The maximum values of the compressive radial stresses for 0.50, 0.75 and 1 mm thicknesses were obtained on the loading axis, and at about 0.6a distance to the loading axis for 0.10 and 0.30 mm thicknesses of the first coating layer. Examining the curves in the contact zone, with increasing in the coating layer thickness, it was seen that the magnitudes of the radial compressive stresses increased until the thickness of 0.50 mm, but decreased after the thickness exceeded the value of 0.50 mm. The magnitudes of the compressive stresses decreased with increasing in the *r/a* ratio, which turned into the tensile stresses near the outside of the contact zone. That tensile stresses reached to the maximum values at the some outside of the contact zone, and then decreased gradually with increasing in the *r/a* ratio. It was observed that the tensile stress values reduced to nearly zero at about 5a distance for all coating layer thicknesses. Although the maximum radial tensile stresses were obtained at the some outside of the contact zone for all coating layer thicknesses, the magnitudes of that maximum stresses were different for each coating layer thickness. Examining the curves in the figure, it was observed that the magnitudes of the maximum radial tensile stresses formed on the contact surface decreased with increasing in the thickness of the first coating layer. The maximum values of σ *r/p** ratios were about 3.247 and 0.647 for the thinnest, 0.10 mm, and the thickest, 1 mm, coating layers, respectively.

Fig.4 shows normalized radial stress distributions along the loading axis for various layer thicknesses of the first coating layer. The radial stresses are equal to Hoop stresses (σθ) along the loading axis. The places where y/y* ratios are zero, 1 and 2 in the figure show the contact surface, the interface between first and second coating layers and the interface between the substrate and first coating layers, respectively. It is seen in the figure that the radial stresses were compressive for all coating layer thicknesses in the contact point (y/y*=0), and the magnitudes of the compressive stresses decreased with increasing in the y/y* ratio.

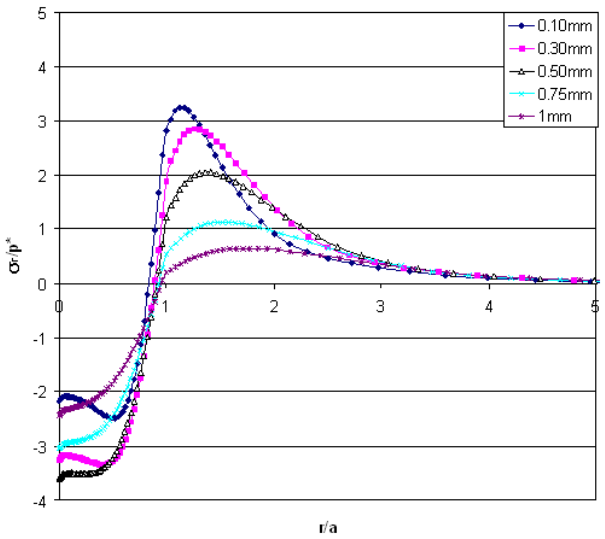

Figure 3. Normalized radial stress distributions for various layer thicknesses of the first coating layer at the contact surface

It was observed that σr/p* ratios became zero, the compressive stresses turned into the tensile stresses, at certain y/y* distances within the coating layer (those y/y* distances were different from each others for different coating layer thicknesses), and, then the curves presented a linear trend until the interface between first and second coating layers. For *y/y*<1* situation (the second coating layer), it was seen that the maximum tensile stress values were obtained at the interface between first and second coating layers. In addition, it was observed that the magnitudes of the stresses decreased with increasing in the thickness of the first coating layer. A sudden decrease in the radial stresses was observed at the interface between first and second coating layers (*y/y*=1*), except for the thickness of 1 mm. In addition, it was seen in the figure that the quantity of the sudden decrease in the stress became less with increase in the first coating layer thickness, and it disappeared for 1mm thickness. That sudden decrease in the stresses considerably characterizes the harmony between the coating layers. The higher the quantity of the sudden decrease in the stress at the interface is, the higher the risk of the failure formation at the interface. Consequently, the risk of the failure formation at the interface between the coating layers decreased with increase in the thickness of the first coating layer.

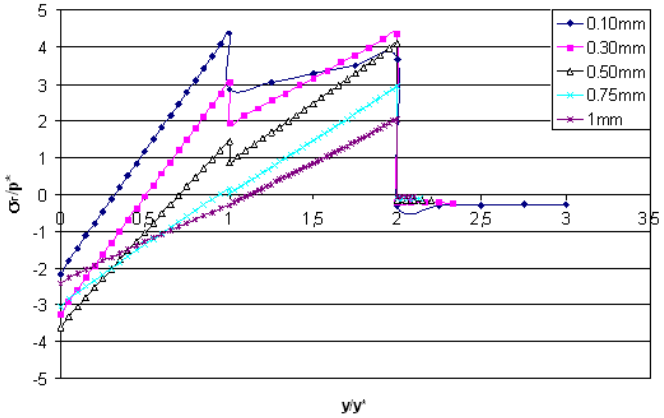

Figure 4. Normalized radial stress distributions for various layer thicknesses of the first coating layer along the loading axis

In addition, as Fig.4 was examined, it is seen that, after the sudden decrease occurred at the radial stresses at the interface between the first and second coating layers (*y/y*=1*), with increasing *y/y** ratio, the tensile stresses continued to increase again until the interface between the first coating layer and substrate (*y/y*=2*), and the maximum tensile stresses were obtained at that interface for *1<y/y*<2*. It can be also seen from the figure that the values of the tensile stresses at the first coating layer decreased with increase in the thickness of that coating layer. A sudden decrease at the radial stresses at the interface between the substrate and the first coating layer (*y/y*=2*) was observed for all thicknesses of the first coating layer. In addition, it is seen in the figure that the amount of the sudden decrease at the stresses at that interface decreases with increase in the thickness of the first coating layer. As a result, it can be said that the risk of failure formation at the interface between the first coating layer and the substrate can be reduced with increase in the thickness of the first coating layer.

Fig.5 shows normalized radial stress distributions at the interface between the first and second coating layers for various layer thicknesses of the first coating layer. Fig.5(a) and Fig.5(b) show the radial stresses on the second and first layer sides, respectively. As the Fig.5(a) and Fig.5(b) were examined, it can be said that, at the symmetry axis (*r/a=0*), the normalized radial stresses at the side of the both coating layers of the interface between the first and second coating layers decreased with increase in the thickness of the first coating layer. In addition, it was observed that the radial stresses at the symmetry axis were tensile for the thicknesses of 0.10-0.75 mm and compressive for the thickness of 1 mm. Examining the figures, it is seen that the radial stress values decreased with increase in the *r/a* ratio for the coating thicknesses of 0.10-0.50 mm. The minimum values in the radial stresses, the maximum compressive stresses, were obtained at the thicknesses of 0.10 and 0.30 mm at the some outside of the contact area.

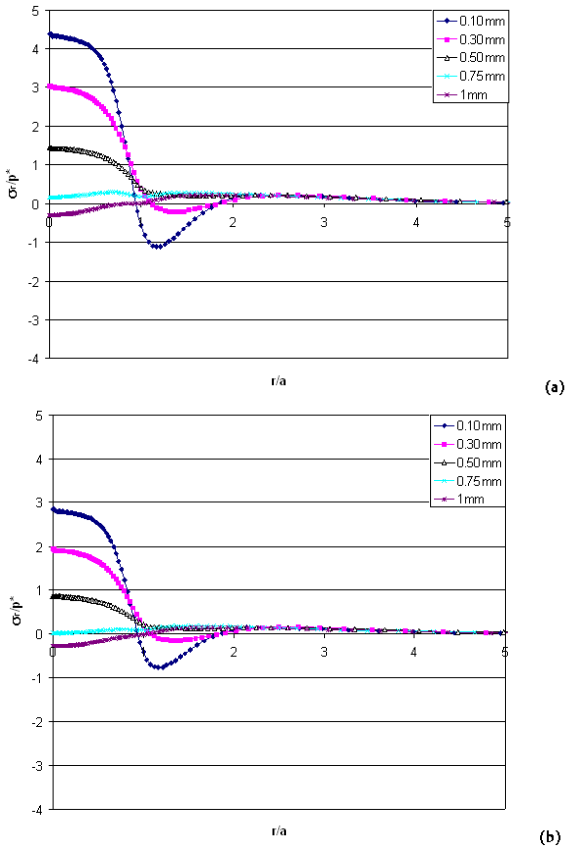

Figure 5. Normalized radial stress distributions at the interface between the first and second coating layers for various layer thicknesses of the first coating layer
a) The second layer side, b) The first layer side

It was observed in the figures that, in the contact area (*r/a<1*), the magnitudes of the radial stresses for the thicknesses of 0.75-1 mm were quite smaller than those of the other coating thicknesses. It can be said that, as the *r/a* ratio exceeded the value of about 2.2, nearly the same radial stresses were obtained for all coating layer thicknesses, that is, the considerable effect of the first coating layer thickness to the radial stresses wasn't observed. As the curves obtained for all coating layer thicknesses were investigated as a whole, it can be said that the risk of failure formation was minimum for thicknesses of the coating layer of 0.75 and 1 mm.

Fig.6 shows normalized radial stress distributions at the interface between the first coating layer and substrate for various layer thicknesses of the first coating layer. Fig.6(a) and Fig.6(b) show the radial stresses on the first coating layer and substrate sides, respectively. As the Fig.6(a) was examined, it can be said that, at the symmetry axis (r/a=0), the normalized radial stresses at the side of the first coating layer of the interface between the first coating layer and substrate decreased with increase in the thickness of the first coating layer. In addition, it was observed that the radial stresses were tensile for every thickness.

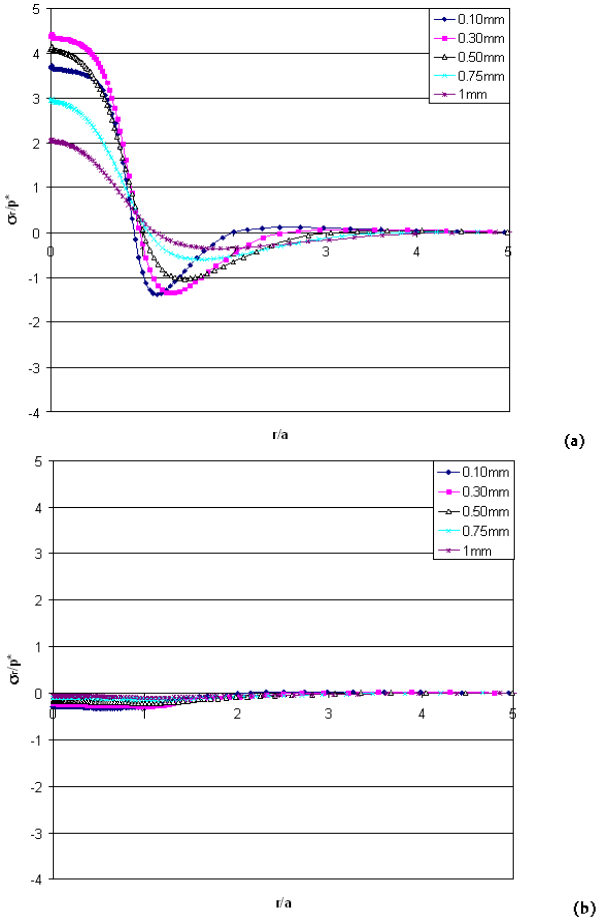

Figure 6. Normalized radial stress distributions at the interface between first coating layer and substrate for various layer thicknesses of the first coating layer
a) The first layer side, b) The substrate side

Examining the figures, it is seen that the radial stress values decreased with increase in the *r/a* ratio. The stresses turned into compressive at about *r/a=1*, and the minimum values in the radial stresses, the maximum compressive stresses, were obtained at the some outside of the contact area for every thickness of the first coating layer. As being gone far from the contact area gradually, with the increase in the *r/a* ratio, it can be said that the values of the compressive stresses decreased and, as the ratio was greater than about 3.7, nearly the same radial stresses were obtained for all coating thicknesses. In addition, it was observed in the figure that the

magnitudes of the radial stresses for the thicknesses of 0.75-1 mm were smaller than those of the other coating thicknesses. As the Fig.6(b) was examined, it can be said that, at the symmetry axis ($r/a=0$), the normalized radial stress values at the side of the substrate of the interface between the first coating layer and the substrate were very low and didn't change considerably with increase in the thickness of the first coating layer. Besides, the increase in r/a ratio didn't affect considerably the radial stresses at the side of the substrate of that interface.

Any decohesion mechanism depends on the presence of a stress gradient and on the sign of the in-plane stresses [15]. When the film is in tension, decohesion initiates preferentially at free edges and propagates inwards, and when the film is under compression, decohesion involves buckling in the film above an initial interface separation, followed by spreading of separated region. Spalling compressive stresses will reduce the risk of tensile failure and increase the risk of buckling, whereas tensile stresses will have the opposite effect [16]. Coating on relatively ductile substrate often fails during indentation by radial and in some cases circumferential crack. Radial or circumferential cracks might initiate from the coating side of the interface and may grow into a through thickness crack [1].

Radial tensile stresses are responsible for the initiation of circumferential cracks, and circumferential tensile stresses are responsible for radial cracks. When the surface stresses are tensile and the interface stresses are compressive, the layer is bent in this region [17].

5. Conclusions

The conclusions obtained through the analysis are listed in the following,

● At the contact surface ($y/y^*=0$), the magnitudes of both tensile and compressive stresses decreased with increase in the first coating layer thickness.

● At the symmetry axis ($r/a=0$), the compressive stresses turned into the tensile stresses at certain y/y^* distances within the coating layer, and those y/y* distances were different from each others for different coating layer thicknesses. In addition, a sudden decrease in the radial stresses was observed at the interfaces, both the first coating layer - second coating layer interface ($y/y^*=1$) and the first coating layer – the substrate interface ($y/y^*=2$). However, at the both interfaces, it was observed that the sudden decrease in the radial stresses decreased with increase in the first coating layer thickness.

● At the interface between the first and second coating layers, the magnitudes of the radial stresses at the both sides of the interface decreased quite with increase in the first coating layer thickness.

● At the interface between the first coating layer and the substrate, the magnitudes of the radial stresses at the coating layer side of the interface decreased quite with increase in the first coating layer thickness. But, at the substrate side of the interface, the magnitudes of the stresses were very small and have near to each others.

As a result, at the double layered coatings, it was obtained that the thickness of the first coating layer (interlayer) affected considerably the stresses formed at the contact surface, the symmetry axis and the interfaces (at the first coating layer – second coating layer and the first coating layer – the substrate), and the magnitudes of the stresses, consequently the risk of the failure formation, decreased importantly with the increase in the thickness of the first coating layer (interlayer).

Declaration of Conflict of Interests

The authors declare that there is no conflict of interest.

References

[1] Abdul-Baqi A, Giessen EVD. Numerical analysis of indentation-induced cracking of brittle coatings on ductile substrates. Int J Solids Struct 2002; 39: 1427-42.

[2] Karimi A, Wang Y, Cselle T, Morstein M. Fracture mechanisms in nanoscale layered hard thin films. Thin Solid Films 2002; 420: 275-80.

[3] Yoo YH, Lee W, Shin H. Spherical nano-indentation of a hard thin film/soft substrate layered system: II. Evolution of stress and strain fields. Model Simul Mater Sc 2004; 12: 69-78.

[4] Sen S, Gun B. A finite element analysis of residual stress at the unloaded stage of the indentation of an elastic-work hardening layered half-space by a rigid sphere. Surf Coat Tech 2006; 200:2841-51.

[5] Komvopoulos K. Finite element analysis of a layered elastic solid in normal contact with a rigid sphere. J Tribol T ASME 1988; 110: 477-85.

[6] Komvopoulos K. Elastic-plastic finite element analysis of indented layered media. J Tribol T ASME 1989; 111: 430-9.

[7] Kral ER, Komvopoulos K, Bogy DB. Indentation of an elastic-plastic layered medium by a rigid sphere, part 1: surface results. J Appl Mech T ASME 1995; 62: 20-8.

[8] Kral ER, Komvopoulos K, Bogy DB. Finite element analysis of repeated indentation of an elastic-plastic layered medium by a rigid sphere, part 2: subsurface. J Appl Mech T ASME 1995; 62: 29-42.

[9] Tangena AG, Wijnhoven PJM. The correlation between mechanical stresses and wear in a layered system. Wear 1988; 121: 27-35.

[10] Tian H, Saka N. Finite element analysis of an elastic-plastic two layer half-space: sliding contact. Wear 1991; 148: 261-85.

[11] Bennani HH, Takadoum J. Finite element model of elastic stresses in thin coatings submitted to applied forces. Surf Coat Tech 1999; 111: 80-5.

[12] Sen S, Aksakal B, Ozel A. A Finite-element analysis of the indentation of an elastic-work hardening layered half – space by an elastic sphere. Int J Mech Sci 1998; 40: 1281-93.

[13] Fouvry S, Wendler B, Liskiewicz T, Dudeka M, Kolodziejczyk L. Fretting wear analysis of TiC/VC multilayered hard coatings: experiments and modelling approaches. Wear 2004; 257: 641-653.

[14] Xia SM, Gao YF, Bower AF, Lev LC, Cheng YT. Delamination mechanism maps for a strong elastic coating on an elastic–plastic substrate subjected to contact loading. Int J Solids Struct 2007; 44: 3685-99.

[15] Djabella H, Arnell RD. Finite-element analysis of the contact stresses in an elastic coating on an elastic substrate. Thin Solid Films. 1992; 213: 205-19.

[16] Arnell RD. Stress-distribution in layered surfaces subjected to tribological forces, Phys Status Solidi A 1994;145: 247-54.

[17] Michler J, Blank E. Analysis of coating fracture and substrate plasticity induced by spherical indenters: diamond and diamond-like carbon layers on steel substrates. Thin Solid Films 2001; 381: 119-34.